

**A MatP-divisome interaction coordinates chromosome segregation with cell division in *E. coli***

Olivier Espéli, Romain Borne, Pauline Dupaigne, Axel Thiel, Emmanuelle Gigant,  
Romain Mercier, and Frédéric Boccard

**Supplementary material**

## Texts and legends of the supplementary figures

### Figure S1. Organization of the MatP foci

**A)** Merged pictures of MatP-mCherry (red) and phase contrast micrographs (gray) of MG1655 cells with a circular chromosome. Only small cells with one or two MatP foci were shown; **B)** quantification of the amount of fluorescence presents in each MatP focus in small cells with two MatP foci.

### Figure S2. MatP holds the ends of a linear chromosome at mid-cell

Snapshot analysis of the localization of the ends of a linear chromosome in the presence or absence of MatP. **A)** Maps of the MKG297 (MG1655 with a circular chromosome) and MKG305 (MG1655 with a linear chromosome) strains. **B)** Merged pictures of the *lacO* array (red), *tetO* array (green) and phase-contrast microscopy (blue) in cells with a circular chromosome (strain MKG297). The percentage of cells presenting mid-cell colocalized *lacO* and *tetO* foci is indicated. **C)** Merged pictures, as in (B), of the *matP* cells with a circular chromosome (MKG297*matP*). **D)** Merged pictures, as in (B), of the cells with a linearized chromosome (MKG305). **E)** Merged pictures, as in (B), of the *matP* cells with a linearized chromosome (MKG305*matP*). **F)** The distance between *tetO* and *lacO* foci from a circular chromosome is moderately increased in the absence of MatP. Histogram of the inter-focal distance between pairs of the closest *lacO* and *tetO* foci according to cell size in MKG297 (blue) and MKG297*matP* (red). **G)** The distance between *tetO* and *lacO* foci from a linear chromosome is dramatically increased in the absence of MatP. Histogram of the inter-focal distance between pairs of the closest *lacO* and *tetO* foci according to cell size in MKG305 (cyan) and MKG305*matP* (orange). **H)** The smallest interfocal distances between pairs of the *lacO* and *tetO* foci were observed when one of the foci was localized at mid-cell. Histograms

of the inter-focal distance between pairs of the closest *lacO* and *tetO* foci according to the position of the *tetO* focus in the strain with circular chromosome MKG297 (blue), MKG297*matP* (red); **I**) Same as (H) for the cells with linear chromosome MKG305 (cyan) and MKG305*matP* (orange). The cells were grown until O.D. 0.2 in minimal medium supplemented with casamino acids, and succinate, arabinose (0.02%), IPTG (50  $\mu$ M) and anhydrotetracycline (50  $\mu$ M) were added 20 min before observation. Scale bar is 3  $\mu$ m.

**Figure S3. Migration of the Ter DNA to mid-cell is not dependent on MatP**

Merged pictures of a time-lapse experiment with 12 min intervals for the segregation of the Ter-3 (red) and Ter-6 (green) loci in strain MG59*matP* (linear chromosome). Seven representative cells are displayed. The purple boxes highlight cells presenting a mid-cell colocalization of the Ter-3 and Ter-6 tags. The full timelapse for these 7 cells corresponds to 67 pictures (1 picture/2min). Scale bar is 3  $\mu$ m.

**Figure S4. Characterization of the replisome pattern in *E. coli* strains with linear chromosome.**

**A)** Measure of the interfocal distance between SSB-Ypet foci in MG58 (circular chromosome), MG58*matP*, MG59 (linear chromosome) and MG59*matP* strains containing two SSB-YPet foci. The histogram corresponds to the average distance in a specific cell size category. This experiment reveals that two categories of cells with two SSB foci are present in the population: small cells (< 3 $\mu$ m) with close SSB-YPet foci and large cells (>3  $\mu$ m) with distant SSB-YPet foci. **B)** Measure of the distance between SSB-YPet and the Ter-2 tag foci in MG59 cells containing only one SSB-YPet focus. The SSB-Ter-2 distance is plotted according to the position of the Ter-2 focus (this graph supports the data presented on Figure 2D). **C)**

Measure of the distances between SSB-YPet and the Ter-2 tag foci in MG59 cells containing two SSB-YPet foci and one ter-2 focus (this graph supports the data presented on Figure 2E). The SSB-Ter-2 distance is plotted according to the position of the Ter-2 focus. For each cell the larger (Maxdist) and smaller (Mindist) distance are plotted.

### **Supplementary text for Figure S5 : Timing of migration to mid-cell for Ter loci depends on their position on the genetic map**

We performed chromosome rearrangements to test directly the influence of the position on the genetic map on the migration of Ter loci. In a strain in which Ter MD has been interrupted by the Right MD, i.e. a large Ter MD region is present at an ectopic position replicated 600 kb earlier (strain FBGT2 in Figure S5A), we analyzed the positioning of three *parS* tags (Right-2, Ter-3 and Ter-6). We focused on small cells presenting only one focus of the tag and analyzed at what cell age it was localized at mid-cell. In wt strains, the small cells presented one Right-2 focus localized either near mid-cell or around the quarter position (Supplementary Figure S5 A-C), as observed previously (Espeli et al. 2008) in agreement with the asymmetric segregation of the replichores (Wang et al. 2006). When cells reached 2.3  $\mu\text{m}$ , every cell presented two Right-2 foci. The new-born cells presented polar Ter-3 and Ter-6 foci. The Ter-3 and Ter-6 loci migrated to mid-cell when the cells reached 3.1  $\mu\text{m}$ , (Supplementary Figure S5B). In the FBGT2 strain (Supplementary Figure S5C), the pattern of localization is altered: a vast majority of the new-born cells presented one Ter-3, one Right-2 and one Ter-6 focus at the pole. The Ter-3 focus is the first to reach mid-cell (before 2.7  $\mu\text{m}$ ). A migration of the Right-2 focus toward mid-cell is observed when the cell reached 3.1  $\mu\text{m}$ . The Ter-6 locus localization remained unchanged; it served as a control and, as expected, its migration timing is unaltered following transposition. Altogether these observations suggested that arrival at mid-cell for a locus in the terminus region can be observed earlier when it was replicated earlier. In a second set of chromosome rearrangements, using a strain with unbalanced replication arms (Esnault et al.

2007), we observed that delaying the replication of a locus from the terminus region (Ter-3 tag) would also delay its timing of migration toward mid-cell (Supplementary Figure S5 D-F). Migration to mid-cell for a locus in the terminus region is therefore coordinated with its replication. Altogether, these results (Figures 4 to 6) show that replication has direct consequences on the sub-cellular positioning of the terminus region during the cell cycle.

### Legend of Figure S5.

**A)** Map of the FBGT2 before and after transposition; the Ori MD (green), NS regions (stripes), Right MD (red), Left MD (dark blue) and Ter MD (cyan) are represented. The positions of the Right-2, Ter-3, Ter-6 and Ter-7 *parS*<sup>P1</sup> tags are represented. The transposition is mediated by the Int + Xis excision of the Right MD from the *attL* and *attR* sites and its subsequent integration into the *attB'* site (Thiel et al., in press). **B)** Cumulative curve representing the presence at mid-cell (position of the focus comprised between 45 and 50% of the cell size) of the Right-2, Ter-3 and Ter-6 loci in the parental FBGT2-NT strain. Only cells with one focus for each tag were taken into account. **D)** Cumulative curves representing the presence at mid-cell (position of the focus comprised between 45 and 50% of the cell size) of the Right-2, Ter-3 and Ter-6 loci in the FBGT2 strain with a transposed Right MD. **D to F)** Analysis of the Ter-3 focus migration to mid-cell following a replication delay imposed by the *terE* Tus binding site inversion **D)** Map of the MG1655 $\Delta$ *terAD* and MG1655 $\Delta$ *terAD-invterE* strains. Inversion of *terE* is mediated by the Int + Xis recombination at the *attL* and *attR* sites. Black arrows represent the replication arms. **E)** Cumulative curve representing the departure from the pole (position of the focus < 30% of the cell size) of the Ter-3 tag. Only cells with one focus for each tag were analyzed. **F)** Histogram of the % of cells present in each category defined by the Ter-3 focus position.

**Figure S6. MatP forms a mid-cell focus colocalized with the septal FtsZ ring protein in a strain with a linear chromosome.**

Merged pictures of MatP-mCherry (red), FtsZ-CFP (cyan) and phase-contrast microscopy (gray) of the MG59 cells grown in minimal medium supplemented with casamino acids and glucose. The percentage of cells with only one MatP focus colocalized with the FtsZ ring or at least one MatP focus colocalized with the FtsZ ring are indicated. (200 cells were counted). Scale bar is 3  $\mu\text{m}$ .

**Figure S7. MatP anchors plasmids with the mats sites to the division septum.**

**A)** Time-lapse experiment representing the dynamics of the pGB2-parST1 plasmid in MG1655. Positioning of the plasmid was observed for 136 min with 1 min intervals. A kymograph of the plasmid fluorescence dynamics in a representative cell (highlighted with a green star) is represented. **B)** Time-lapse experiment representing the dynamics of the pGB2-parST1-2matS plasmid in MG1655. Positioning of the plasmid was observed for 116 min with 1 min intervals. A kymograph of the plasmid fluorescence dynamics in a representative cell (highlighted with a green star) is represented. **C)** Characteristic field of the localization of the pGB2-parST1-2matS plasmid in the AB1157 strain. **D)** Time-lapse experiment representing the dynamics of the pGB2-parST1-2matS plasmid in MG1655*matP*. Positioning of the plasmid was observed for 81 min with 1 min intervals. A kymograph of the plasmid fluorescence dynamics in a representative cell (highlighted with a green star) is represented. **E)** Time-lapse experiment representing the dynamics of the pGB2-parST1-2matS plasmid in MG1655*zapB*. Positioning of the plasmid was observed for 136 min with 1 min intervals. A kymograph of the plasmid fluorescence dynamics in a representative cell (highlighted with a red star) is represented.

**Figure S8. Influence of the *zapA*, *zapB* and *zapC* deletions on the MatP-mCherry localization**

For each strain, a representative field and an histogram of the relative position of the MatP-mCherry foci according to cell size are displayed (about 200 cells were counted for each strain). Scale bar is 3  $\mu\text{m}$ .

**Figure S9. Influence of the *zapB* deletion on the Ter-3 tag localization**

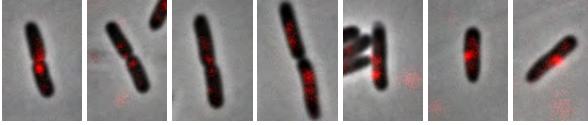
A) Histogram representing the Ter-3 foci localization according to the cell size of the MG1655 strain (200 cells were counted). B) Histogram representing the Ter-3 foci localization according to the cell size of the MG1655*zapB* strain (200 cells were counted). C) Representative picture of the colocalization between MatP-mCherry (red) and the Ter-3 tag (yellow) in MG1655*matP-mcherry* strain D) Representative picture of the colocalization between MatP-mCherry and the Ter-3 tag in MG1655*zapB matP-mcherry* strain. The percentage of colocalized Ter-3 and MatP foci (Inter focal distance <100nm) is indicated. Scale bar is 3  $\mu\text{m}$ .

**Table S1. Strains and plasmids**

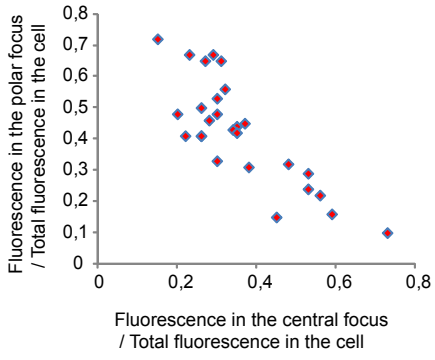
Strain	Description	Reference
MG1655	Lab collection	
MG1655 matP-mcherry :: kan	<i>matP-mcherry::frrt-kn-frrt</i>	Mercier et al., 2008
RM1	MG1655 $\Delta$ <i>matP::frrt-cat-frrt</i>	Mercier et al., 2008
RM2	MG1655 $\Delta$ <i>matP</i>	Mercier et al., 2008
MG1655 matP-mcherry :: rif	<i>matP-mcherry::frrt-rif-frrt</i>	This work
MG58	MG1655 -3kbfif ::tos-kan (circular chromosome)	Gift from T. Horiushi
MG59	MG1655 -3kbfif ::tos-kan , N15 (linear chromosome)	Gift from T. Horiushi
MG58 matP-mcherry	<i>MG58 matP-mcherry::frrt-rif-frrt</i>	This work
MG59 matP-mcherry	<i>MG59 matP-mcherry::frrt-rif-frrt</i>	This work
MG58 <i>matP</i> ::rif	<i>MG58 <math>\Delta</math>matP::frrt-rif-frrt</i>	This work
MG59 <i>matP</i> ::rif	<i>MG59 <math>\Delta</math>matP::frrt-rif-frrt</i>	This work
MG58 <i>matP</i>	<i>MG58 <math>\Delta</math>matP</i>	This work
MG59 <i>matP</i>	<i>MG59 <math>\Delta</math>matP</i>	This work
MKG297	MG58 [ <i>lacO240-Cm</i> ]1567 +[ <i>tetO240-Gm</i> ]1607, <i>yajR::</i> (pBAD:: <i>lacI-cfp tetR-yfp</i> )	Cui et al., 2007
MKG305	MG59 [ <i>lacO240-Cm</i> ]1567 +[ <i>tetO240-Gm</i> ]1607, <i>yajR::</i> (pBAD:: <i>lacI-cfp tetR-yfp</i> )	Cui et al., 2007
MKG297 <i>matP</i> ::rif	<i>MKG297 <math>\Delta</math>matP::frrt-rif-frrt</i>	This work
MKG305 <i>matP</i> ::rif	<i>MKG305 <math>\Delta</math>matP::frrt-rif-frrt</i>	This work
MG582S2	MG58 <i>ydaA::parS</i> (P1) (Ter3), <i>gusC::parS-frrt-cat-frrt</i> (pMT1) (Ter6)	This work
MG582S2 <i>matP</i>	<i>MG582S2 <math>\Delta</math>matP::frrt-rif-frrt</i>	This work
MG592S2	MG59 <i>ydaA::parS</i> (P1) (Ter3), <i>gusC::parS-frrt-cat-frrt</i> (pMT1) (Ter6)	This work
MG592S2 <i>matP</i>	<i>MG592S2 <math>\Delta</math>matP::frrt-rif-frrt</i>	This work
MG582S8	MG58 <i>yocA::parS</i> (pMT1) (Ter7), <i>gusC::parS-frrt-cat-frrt</i> (P1) (Ter6)	This work
MG582S8 matP-mcherry	MG58 <i>yocA::parS</i> (pMT1) (Ter7), <i>gusC::parS-frrt-cat-frrt</i> (P1) (Ter6), <i>matP-mcherry::frrt-rif-frrt</i>	This work
AB1157 <i>ssb-yfpet</i>	<i>ssb-yfpet::frrt-cat-frrt</i>	Reyes-Lamothe et al., 2008
MG1655 <i>ssb-yfpet</i>	<i>ssb-yfpet::frrt-cat-frrt</i>	Mercier et al., 2008
MG1655 <i>ssb-yfpet</i> ::rif	<i>ssb-yfpet::frrt-cat-frrt::rif</i>	This work
MG58 <i>ssb-yfpet</i>	<i>MG58 ssb-yfpet::frrt-cat-frrt::rif</i>	This work
MG58 <i>matP</i> <i>ssb-yfpet</i>	<i>MG58 matP, ssb-yfpet::frrt-cat-frrt::rif</i>	This work
MG59 <i>ssb-yfpet</i>	<i>MG59 ssb-yfpet::frrt-cat-frrt::rif</i>	This work
MG59 <i>matP</i> <i>ssb-yfpet</i>	<i>MG59 matP, ssb-yfpet::frrt-cat-frrt::rif</i>	This work
MG592S7 <i>ssb-yfpet</i>	MG59 <i>yocA::parS</i> (pMT1) (Ter7), <i>osmB::parS-frrt-cat-frrt</i> (P1) (Ter2), <i>ssb-yfpet::frrt-cat-frrt::rif</i>	This work
FBGT2 NT	MG1655 $\Delta$ <i>lacZ</i> , ' <i>lacZ::attL</i> (1099533), <i>lacZ'</i> :: <i>attR</i> (651775), <i>attB'</i> (1533248kb)	This work
FBGT2 transposed	MG1655 $\Delta$ <i>lacZ</i> , <i>lacZattB</i> (651775), <i>attL'</i> (1099533), <i>attR'</i> (1533248)	This work
FBGT2 NT Ter-3	<i>ydaA::parS-frrt-cat-frrt</i> (P1) (Ter3)	This work
FBGT2 NT Right-2	<i>ybfD::parS-frrt-cat-frrt</i> (P1) (Right2)	This work
FBGT2 NT Ter-6	<i>gusC::parS-frrt-cat-frrt</i> (P1) (Ter6)	This work
MG1655 intra-R3 ni	MG1655 $\Delta$ <i>lacZ <math>\Delta</math>terAD</i>	Esnault et al., 2007
MG1655 intra-R3 i	MG1655 $\Delta$ <i>lacZ <math>\Delta</math>terAD invterE</i>	Esnault et al., 2007
AB1157 <i>dnaBts</i>	<i>dnaBts</i> :: <i>tc</i>	Gift from B. Michel
MG582S2 <i>dnaBts</i>	MG582S2 <i>dnaBts</i> :: <i>tc</i>	This work
MG582S8 <i>dnaCts</i>	MG582S8 <i>dnaCts</i> :: <i>tc</i>	This work
MG1655 <i>ftsZ84</i>	Transduced from AB1157 <i>ftsZ84</i> , <i>leu2</i> :: <i>kan</i>	This work

MG1655zapA	$\Delta$ zapA:: <i>frt-kan-frt</i> transduced from keio collection	This work
MG1655zapB	$\Delta$ zapB:: <i>frt-kan-frt</i> transduced from keio collection	This work
MG1655zapC	$\Delta$ zapC:: <i>frt-kan-frt</i> transduced from keio collection	This work
MG1655zipAts	<i>zipAts</i> ::kan	This work
MG1655ftsAts	Transduced from AB1157 <i>ftsAts</i> , <i>leu2</i> ::kan	This work
MG1655ftsIts	Transduced from AB1157 <i>ftsIts</i> , <i>leu2</i> ::kan	This work
MG1655ftsK $\Delta$ C ::cam	Transduced from DS9041	Gift from D. Sherratt
MG1655 matP-mcherry zapB	$\Delta$ zapB:: <i>frt-kan-frt</i> transduced from keio collection	This work
MG1655 matP-mcherry zapA	$\Delta$ zapA:: <i>frt-kan-frt</i> transduced from keio collection	This work
MG1655 matP-mcherry zapC	$\Delta$ zapC:: <i>frt-kan-frt</i> transduced from keio collection	This work
MG1655 matP zapA	$\Delta$ zapA:: <i>frt-kan-frt</i> transduced from keio collection in RM2	This work
MG1655 matP zapB	$\Delta$ zapB:: <i>frt-kan-frt</i> transduced from keio collection in RM2	This work
BTH101	<i>F- cya-99 araD139 galE15 galK16 rpsL1 (Strr) hsdR2 mcrA1 mcrB1</i>	Gift from D. Ladent
BTH101zapA::kan	$\Delta$ zapA:: <i>frt-kan-frt</i> transduced from keio collection	This work
BTH101zapA	BTH101zapA::kan without the kan resistance gene	This work
<b>Plasmids</b>	<b>Description</b>	<b>Reference</b>
pFH2973	CFP- $\Delta$ 30ParBP1/ YFP- $\Delta$ 23ParBT1 expression vector	Nielsen et al., 2006b
pALA2705	GFP- $\Delta$ 30ParBP1 expression vector	Li et al., 2003
pTSA29CXI	pTSA29 carrying cI857-P <sub>R</sub> (xis -int )	Valens et al., 2004
pGBM2-parST1	pGBM2 carrying the parS(pMT1) tag	This work
pGBM2-parST1-1matS	pGBM2-parST1 carrying 1Kb of genomic DNA with matS15	This work
pGBM2-parST1-2matS	pGBM2-parST1 carrying 1Kb of genomic DNA flanked by <i>matS15</i> and a second <i>matS</i> site	This work
pEG3A	pACYC99A, PBAD: <i>egfp-zapB</i>	Gift from K. Gerdes
pCP7 ftsZ-CFP	FtsZ-CFP controlled by a weak constitutive promoter	Gift from D. Sherratt
pBAD24 zapA-GFP	pBAD24, PBAD: <i>egfp-BamHI-zapA</i> fusion cloned into pBAD24 NcoI-HindIII	This work
pKD3	template plasmid <i>frt-cat-frt</i>	Datsenko and Wanner, 2000
pKD4	template plasmid <i>frt-Kn-frt</i>	Datsenko and Wanner, 2000
pGBKD3-parSP1	pGB2 carrying <i>frt-cat-frt</i> from pKD3 upstream from <i>parS</i> (P1)	Espéli et al., 2008
pGBKD3-parSpMT1	pGB2 carrying <i>frt-cat-frt</i> from pKD3 upstream from <i>parS</i> (pMT1)	Mercier et al., 2008
pGBKD3-rif	template plasmid <i>frt-rif-frt</i>	This work
pUT18c	Bacterial two hybrid vector 1	Gift from D. Ladent
pUT18cmatP <sub>c90</sub>	<i>matP</i> deleted of the 267 first pb cloned into pUT18c	This work
pKT25	Bacterial two hybrid vector 2	Gift from D. Ladent
pKT25matP	<i>matP</i> cloned into pKT25	This work
pKT25zapA	zapA cloned BamHI-PstI into pKT25	This work
pKT25zapB	zapB cloned BamHI-PstI into pKT25	This work
pKT25zapBA6	zapB deleted from the last 18pb cloned BamHI-PstI into pKT25	This work
pKT25zapBA11	zapB deleted from the last 33pb cloned BamHI-PstI into pKT25	This work
pKT25zapBL-G	zapB with mutations converting the last 3 leucines of ZapB into glycines cloned BamHI-PstI into pKT25	This work

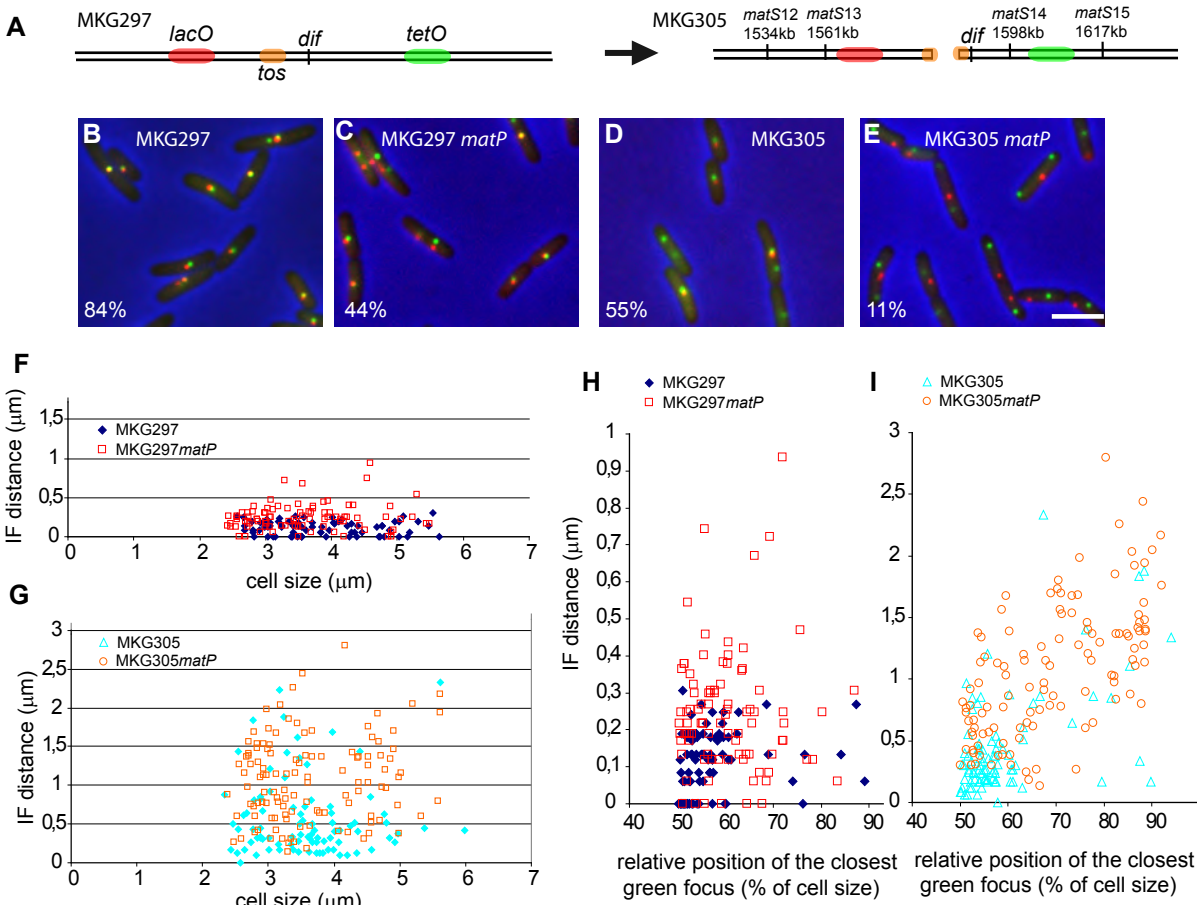
A



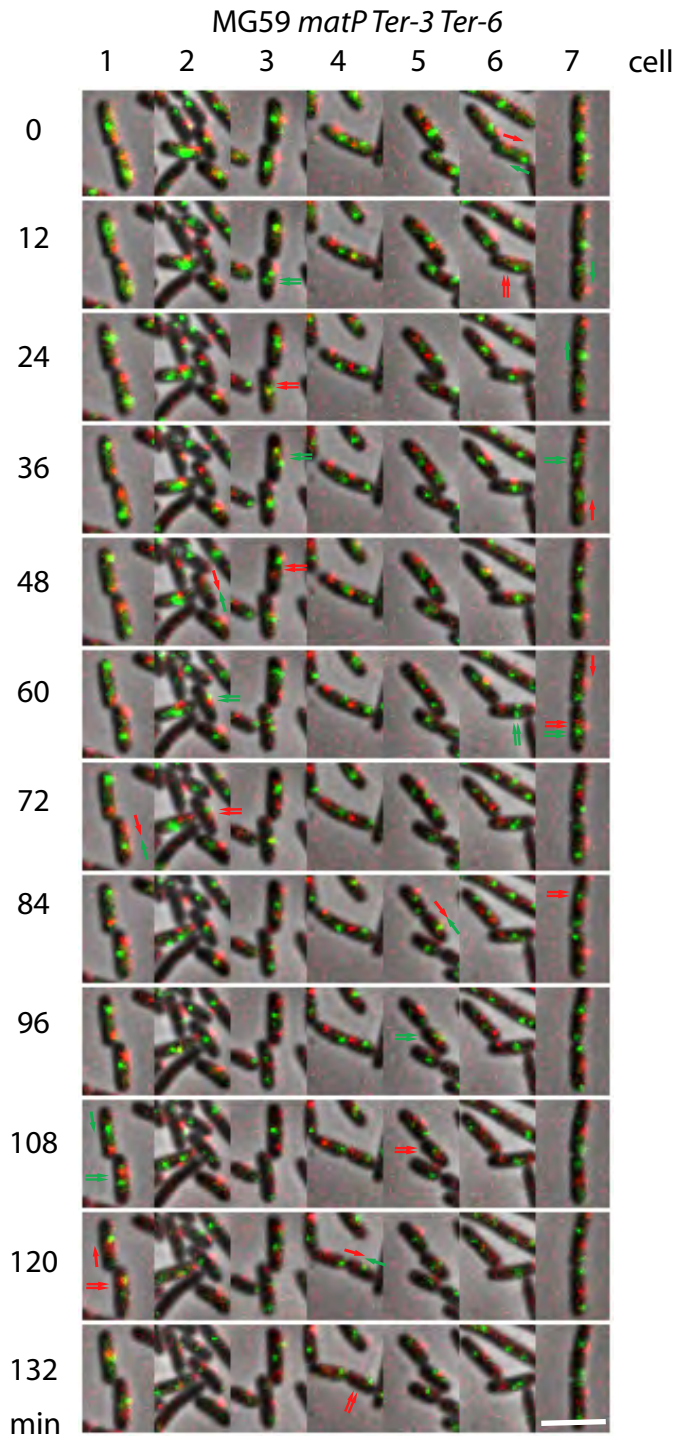
B



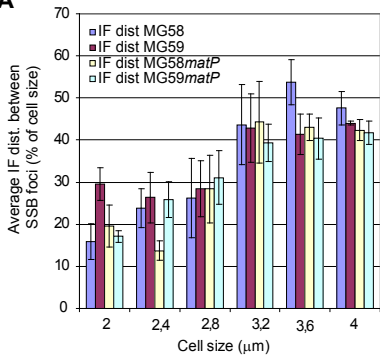
Espéli\_Supplementary Fig S1.



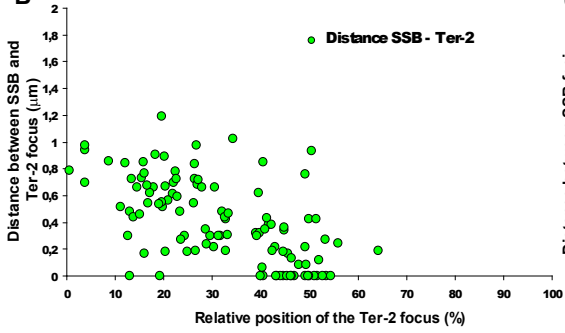
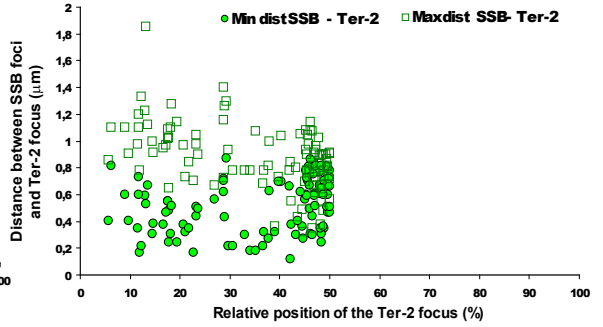
Espéli\_Supplementary Fig. S2

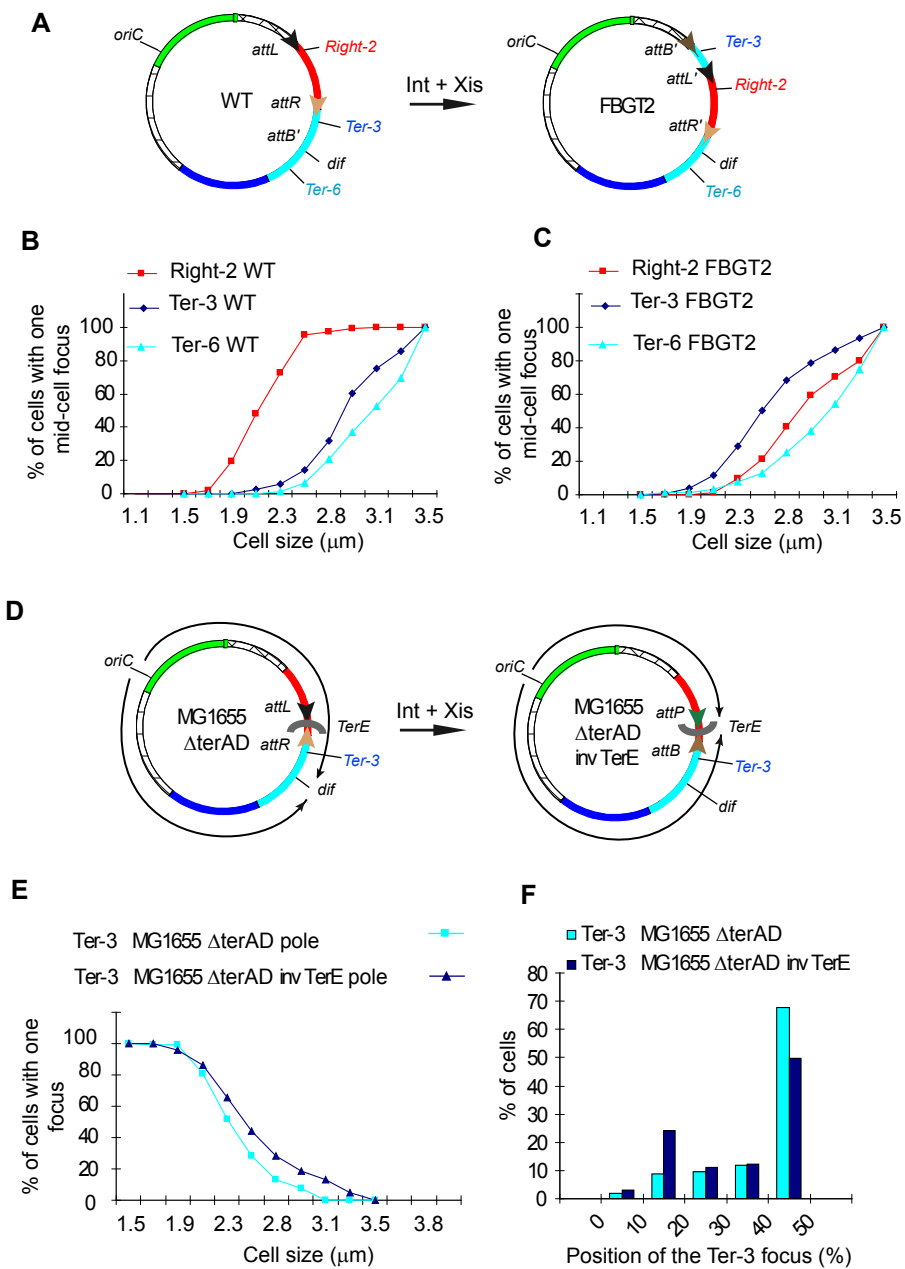


Espéli\_Supplementary Fig. S3

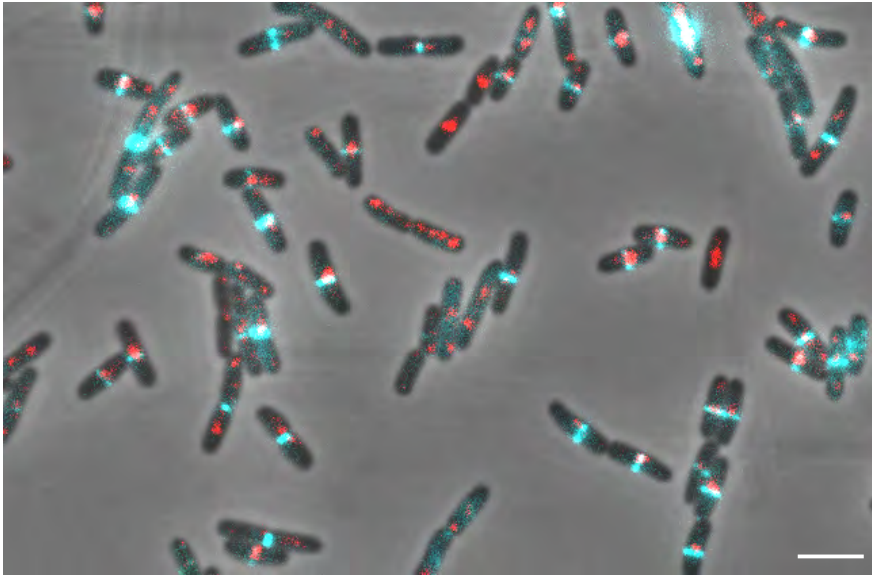
**A**

Espéli\_Supplementary Fig. S4

**B****C**

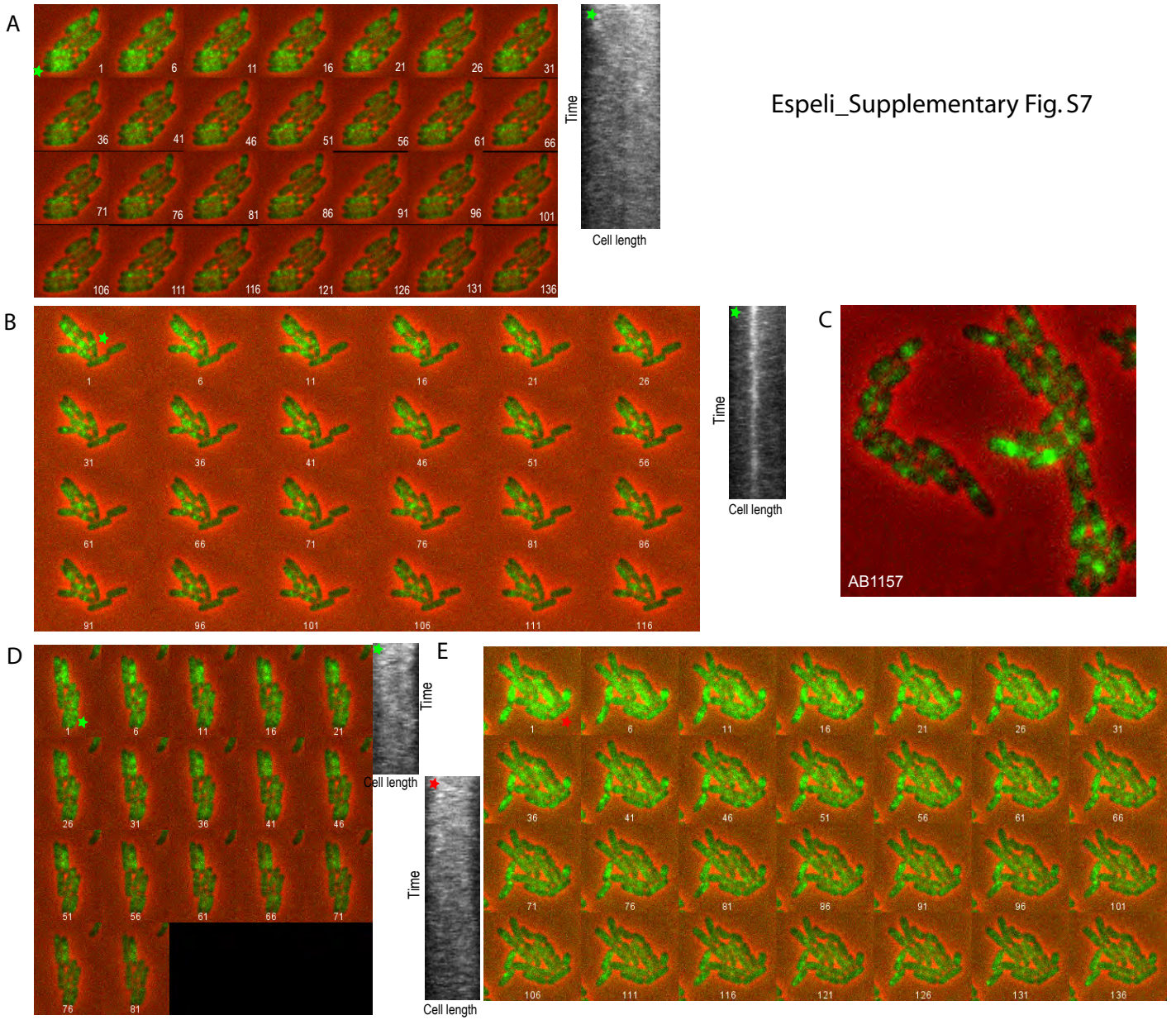


Espeli\_Supplementary Fig.S5

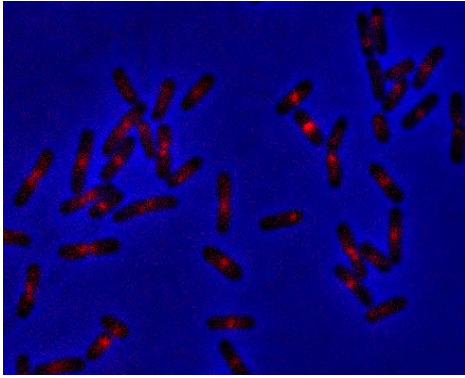


27% of the cells present only one MatP-mCherry focus and one FtsZ-CFP ring colocalized at mid-cell  
60% of the cells present one of the MatP-mCherry foci and one FtsZ-CFP ring colocalized at mid-cell

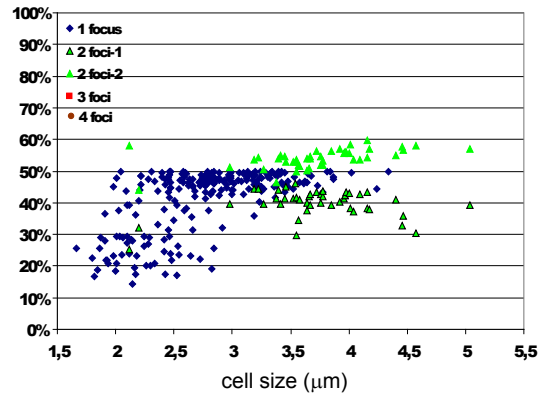
Espéli\_Supplementary Fig. S6



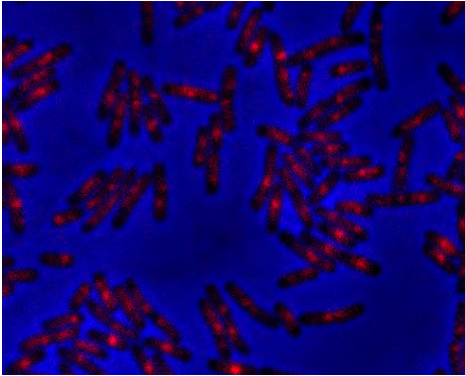
MG1655 *matP*-cherry



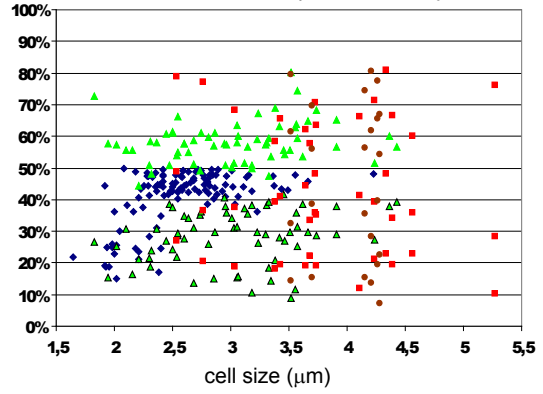
MG1655 *matP*-cherry



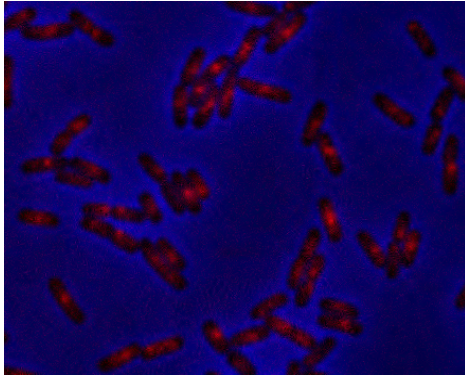
MG1655 *zapA* *matP*-cherry



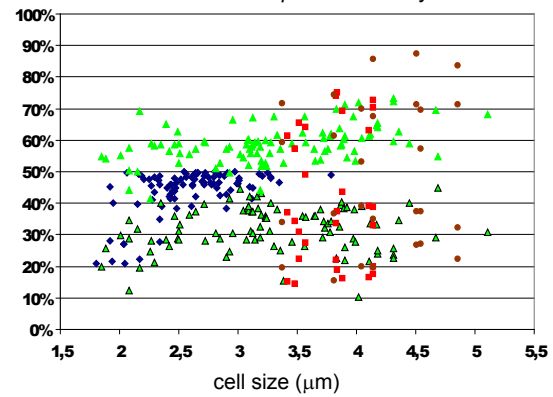
MG1655 *zapA* *matP*-cherry



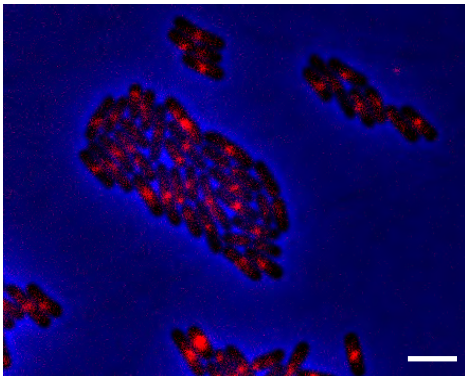
MG1655 *zapB* *matP*-cherry



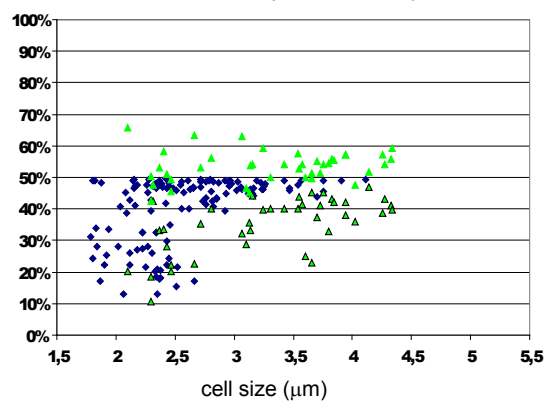
MG1655 *zapB* *matP*-cherry

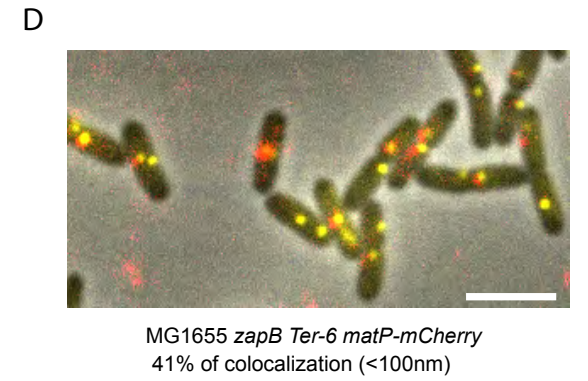
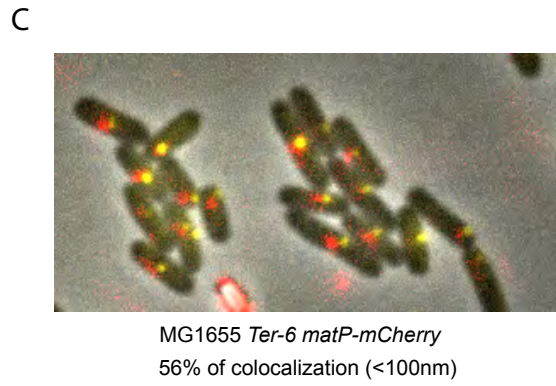
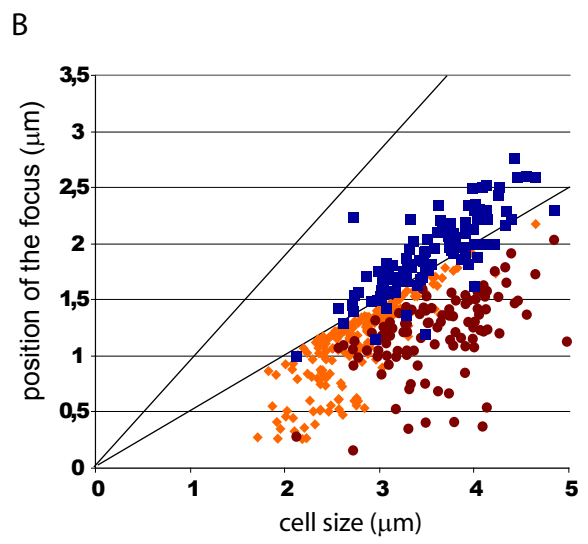
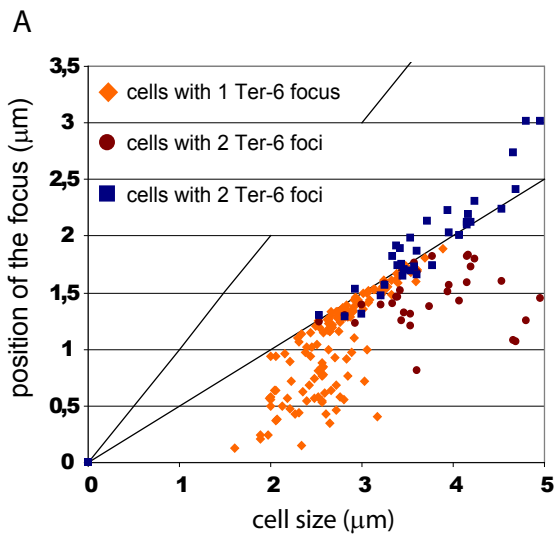


MG1655 *zapC* *matP*-cherry



MG1655 *zapC* *matP*-cherry





Espéli\_Supplementary Fig. S9